Contribution from the Departments of Chemistry, Northeastern University, Boston, Massachusetts 02115, and Brandeis University, Waltham, Massachusetts 02154

The Ferric Chloride–α-Diamine System. 3. X-ray Crystallographic, Magnetic Susceptibility, and Zero- and High-Field Mössbauer Spectroscopy Investigation of $[Fe(2,2'\text{-bpy})_2Cl_2][FeCl_4]$: Slow Paramagnetic Relaxation and Magnetic Ordering of Complex Bimetallic Salts

Edward H. Witten,[†] William M. Reiff,*[†] K. Lázár,[†] Brian W. Sullivan,[‡] and Bruce M. Foxman*[‡]

Received November 14, 1984

The title compound crystallizes in the orthorhombic space group $P2_12_12_1$, $Z = 4$, with $a = 11.707$ (4) Å, $b = 12.038$ (4) Å, and $c = 18.308$ (7) Å. The structure consists of discrete linear arrays of alternating $[Fe(bpy)_2Cl_2]^+$ cations and $[FeCl_4]^-$ anions located at intervals of $\sim c/2$ in the unit cell. The shortest interionic contact (Cl–C) is 3.39 Å. The $[Fe(bpy)_2Cl_2]^+$ ion forms a distorted octahedron with the two chlorine atoms in a cis arrangement. A significant lengthening is observed for those Fe–N distances trans to Cl (average 2.193 (7) Å; Fe–N cis to Cl average 2.121 (9) Å). The $[FeCl_4]^-$ ion displays the expected tetrahedral geometry with Fe–Cl = 2.184 (2) Å. Low-temperature magnetic susceptibility and Mössbauer spectra in zero and various applied fields suggest a complex combination of slow paramagnetic relaxation and weak magnetic order in the range 10–1 K.

Introduction

In recent years there has been considerable emphasis on magnetostructural correlations for a variety of magnetically one- and two-dimensional chain polymer and layer compounds.[1,2] The strongest magnetic interactions in these systems are usually transmitted by bonded bridging ligand atoms or groups as part of a mechanism generally referred to as superexchange. There have been relatively few studies of the cooperative, long-range magnetic ordering of complex salts containing large multiatom cations and anions. Representative systems for the case of high-spin iron(III) typically contain the very stable tetrachloroferrate anion, e.g. $[(CH_3)_4N][FeCl_4]$[3] and $[2,9\text{-}(CH_3)_2phenH][FeCl_4]$.[4] The magnetic interactions in these compounds are weak ($T_{Néel} < 4.2$ K). This is not unexpected in view of the absence of formal bridging ligands connecting the $[FeCl_4]^-$ tetrahedra. On the other hand, we have recently characterized[5,6] a complex hexachloroferrate $[Co(pn)_3][FeCl_6]$ (pn = 1,2-propanediamine) and find it to be a cubic, three-dimensional antiferromagnet having a surprisingly high Néel temperature (~9 K). In all of the foregoing complex salts, the paramagnetism resides in the complex anion sublattice. We have extended these studies to a new polymorph of $[Fe(2,2'\text{-bpy})_2Cl_2][FeCl_4]$ and $[Fe(cp)_2][FeCl_4]$. The former contains both the spin-sextet cation and anion while the latter contains the spin-doublet ferrocenium cation along with the spin-sextet anion.

The advantage of the Mössbauer effect in these investigations is that it is uniquely capable of exhibiting both cooperative ordering and slow paramagnetic relaxation. The ($S = {}^5/_2$, $S = {}^5/_2$) system presented herein exhibits a complex combination of these phenomena in the temperature range 10–1 K while our preliminary results for the $S = {}^1/_2$, $S = {}^5/_2$ system indicate similar behavior in the range 4–1 K. The results of these investigations have been reported previously in preliminary form.[7]

Experimental Section

The Mössbauer spectra were determined by using a standard constant acceleration spectrometer for which the source (106 mCi Co^{57} in Rh) was always at ambient temperature. Temperature measurement was based on either a calibrated silicon or gallium arsenide diode or helium vapor pressure thermometry as described previously.[8] The details of the Faraday susceptibility apparatus have also been described. The polymorph of $[Fe(2,2'\text{-bpy})_2Cl_2][FeCl_4]$ considered here was obtained via crystallization of what is believed to be a polymeric isomer, $[Fe(2,2'\text{-bpy})Cl_2]_\infty Cl_\infty$, from acetone or nitromethane solutions; the products so obtained gave the expected chemical analysis (from acetone). Anal. Calcd: C, 37.72; H, 2.53; N 8.80. Found: C, 38.11; H, 2.26; N, 8.63.

The polymer isomer is obtained as a *polycrystalline product* via rapid precipitation that results on the mixing of small volume (~20 mL) solutions of *anhydrous* ferric chloride in *anhydrous* methanol with similar small volume solutions of *anhydrous* ligand in *anhydrous* methanol in ~1:1 metal to ligand stoichiometry. The latter polymeric isomer is apparently a kinetically favored species. We find that further physico-

Table I. Data for the X-ray Diffraction Study of $[Fe(bpy)_2Cl_2]^+[FeCl_4]^-$

(A) Crystal Data at 21 (1) °C

cryst syst: orthorhombic	$Z = 4$
space group: $P2_12_12_1$ [D_2^4, No. 19]	cryst size: 0.13 × 0.17 × 0.25 mm
$a = 11.707$ (4) Å	fw: 636.8
$b = 12.038$ (4) Å	$\rho_{calcd} = 1.64$ g/cm^3
$c = 18.308$ (7) Å	$\rho_{obsd} = 1.63$ g/cm^3
$V = 2580.1$ Å^3	$\mu = 17.9$ cm^{-1}

cell const determ: 11 pairs of $\pm(hkl)$ and refined 2θ, ω, and χ values in the range $24° < |2\theta| < 25°$.

(B) Measurement of Intensity Data[a]

radiation: Mo Kα, graphite monochromator
reflcns measd $+h,+k,+l$ (to $2\theta = 43°$)
scan type; speed: θ–2θ; 1.95–3.91°/min
scan range: symmetrical, $[1.6 + \Delta(\alpha_2 - \alpha_1)]°$
bkgd meas: ${}^1/_4$ of scan time at each of the scan limits
no. of reflcns measd: 1720
std reflcns: 172, 633, 004; period 50, variation $\leq 3\sigma(I)$ for each
abs cor: empirical, transmission factors 0.89–1.00
statistical info: $R_s = 0.038$

(C) Solution and Refinement[b,c]

solution: direct methods (MULTAN) and difference Fourier
refinement: anisotropic temperature factors for Fe and Cl atoms; isotropic temperature factors for N, C, and H atoms; $R = 0.046$, $R_w = 0.053$; SDU = 1.032
final structure factor calcns for all 1720 data: $R = 0.080$; $R_w = 0.059$
final difference map: largest peak, 0.45 e/Å^3 near C(8); one peak, 0.40 e/Å^3 near C(18); all other peaks random and ≤0.32 e/Å^3

[a] $R_s = \sum\sigma(|F_o|)/\sum|F_o|$. [b] $R = \sum||F_o| - |F_c||/\sum|F_o|$; $R_w = [\sum w(|F_o| - |F_c|)^2/\sum w|F_o|^2]^{1/2}$; SDU = $[\sum w(|F_o| - |F_c|)^2/(m - n)]^{1/2}$, where m (1241) is the number of observations and n (169) is the number of parameters. [c] For 1241 data, $F > 3.92\sigma(F)$.

(1) De Jongh, L. J.; Miedema, A. R. *Adv. Phys.* **1976**, *23*, 1.
(2) Steiner, M.; Villain, J.; Windsor, G. G. *Adv. Phys.* **1976**, *25*, 87.
(3) Edwards, P. R.; Johnson, C. E. *J. Chem. Phys.* **1968**, *4*, 211.
(4) Veidis, M. V.; Witten, E. H.; Reiff, W. M.; Brennan, T. F.; Garafalo, A. R. *Inorg. Chim. Acta* **1981**, *54*, L133.
(5) Reiff, W. M.; Scoville, A. N.; Witten, E. H. "Abstracts of Papers", 179th National ACS Meeting, Houston, TX, March 1980; American Chemical Society: Washington, DC, 1980; NUCL 58.
(6) Scoville, A. N.; Reiff, W. M.; Landee, C. *Inorg. Chem.* **1983**, *22*, 3514.
(7) (a) Witten, E. H.; Reiff, W. M.; Sullivan, B. W.; Foxman, B. M. "Abstracts of Papers", 182nd National ACS Meeting, New York, NY, Aug 1981; American Chemical Society: Washington, DC, 1981; INOR 133. (b) Reiff, W. M.; Lázár, K.; Landee, C. "Abstracts of Papers", 188th National ACS Meeting, Philadelphia, PA, Aug 1984; American Chemical Society: Washington, DC, 1984; INOR 159.

[†] Northeastern University.
[‡] Brandeis University.

0020-1669/85/1324-4585$01.50/0

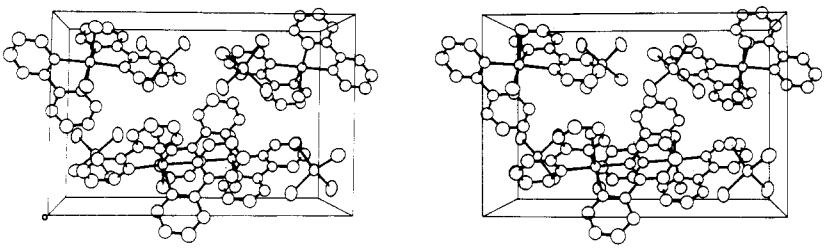

Figure 1. Stereoview of the crystal structure of $[Fe(bpy)_2Cl_2]^+[FeCl_4]^-$ (*b* vertical, *c* horizontal).

Table II. Atomic Coordinates[a] for $[Fe(bpy)_2Cl_2]^+[FeCl_4]^-$

atom	*x*	*y*	*z*
Fe(1)	0.0565 (2)	0.24576 (14)	0.37114 (9)
Fe(2)	0.0119 (2)	0.22571 (15)	0.87000 (10)
Cl(1)	0.2036 (3)	0.1252 (3)	0.3748 (10)
Cl(2)	0.1478 (3)	0.4082 (3)	0.3513 (2)
Cl(3)	−0.1252 (4)	0.3047 (3)	0.9320 (2)
Cl(4)	0.1188 (4)	0.1265 (4)	0.9427 (2)
Cl(5)	0.1140 (4)	0.3543 (3)	0.8166 (2)
Cl(6)	−0.0631 (4)	0.1160 (4)	0.7881 (2)
N(1)	0.0114 (10)	0.2260 (9)	0.2598 (5)
N(2)	−0.1086 (9)	0.3309 (8)	0.3595 (5)
N(3)	−0.0558 (9)	0.1081 (8)	0.4017 (5)
N(4)	0.0405 (9)	0.2593 (9)	0.4862 (5)
C(1)	0.0812 (12)	0.1709 (11)	0.2119 (7)
C(2)	0.0517 (14)	0.1641 (12)	0.1379 (8)
C(3)	−0.0416 (13)	0.2181 (11)	0.1154 (8)
C(4)	−0.1106 (12)	0.2790 (12)	0.1620 (8)
C(5)	−0.0808 (11)	0.2802 (10)	0.2347 (6)
C(6)	−0.1474 (12)	0.3386 (10)	0.2903 (7)
C(7)	−0.2482 (12)	0.3958 (11)	0.2741 (7)
C(8)	−0.3074 (13)	0.4444 (12)	0.3294 (8)
C(9)	−0.2708 (13)	0.4365 (11)	0.4005 (7)
C(10)	−0.1703 (12)	0.3773 (10)	0.4132 (7)
C(11)	−0.0998 (12)	0.0316 (11)	0.3556 (7)
C(12)	−0.1619 (12)	−0.0569 (10)	0.3824 (8)
C(13)	−0.1753 (13)	−0.0700 (13)	0.4552 (8)
C(14)	−0.1321 (13)	0.0071 (11)	0.5025 (7)
C(15)	−0.0729 (12)	0.0994 (11)	0.4747 (6)
C(16)	−0.0260 (11)	0.1855 (10)	0.5209 (7)
C(17)	−0.0493 (13)	0.1969 (11)	0.5946 (7)
C(18)	−0.0022 (13)	0.2834 (12)	0.6338 (8)
C(19)	0.0682 (14)	0.3547 (12)	0.6001 (8)
C(20)	0.0878 (13)	0.3426 (11)	0.5248 (7)

[a] Standard deviations in the least significant digit appear in parentheses.

chemical manipulation of this material leads to the formation of other more thermodynamically stable isomers such as the complex bimetallic salt detailed herein. The structural and magnetic properties of the polymeric $[Fe(bpy)Cl_2]_\infty Cl_\infty$ are completely different than those of the title compound and are the subject of a subsequent article.

We have found that we can also obtain the compound in analytically pure, polycrystalline powder form via the thermolysis 2[2,2′-bpyH]-$[FeCl_4]$(s) → $[Fe(2,2'\text{-bpy})_2Cl_2][FeCl_4]$(s) + 2HCl(g). Debye–Scherrer X-ray powder patterns show that the materials used for susceptibility and Mössbauer spectroscopy analyses are isomorphous to that used for structure determination.

Crystals of the title complex were grown by slow evaporation from nitromethane. Operations on the Syntex $P2_1$ diffractometer and XTL structure determination system were carried out as described previously.[9] The small size and poor diffraction quality of even the best crystals limited the data collection to $2\theta \leq 43°$ using Mo Kα radiation; few reflections with $I/\sigma(I) > 3$ were observed at greater values of 2θ. Essential details of the structure analysis, in outline form, are given in Table I. The results presented in Tables I and II (atomic coordinates) represent refinement of the correct crystal chirality; for the structure of opposite chirality, least-squares refinement led to $R = 0.049$ and $R_w = 0.058$.

Table III. Selected Nonbonded Contacts[a]

atom pair	dist, Å	symmetry operation
Cl(1)–Cl(4)	3.880	$^1/_2 - x, y, z - ^1/_2$
Cl(2)–Cl(5)	4.044	$^1/_2 - x, 1 - y, z - ^1/_2$
Cl(2)–Cl(6)	4.248	$^1/_2 + x, ^1/_2 - y, 1 - z$
Cl(3)–Cl(4)	3.864	$x - ^1/_2, ^1/_2 - y, 2 - z$
Cl(5)–Cl(6)	3.735	$x, ^1/_2 + y, ^3/_2 - z$
Cl(1)–C(17)	3.643	$^1/_2 + x, ^1/_2 - y, 1 - z$
Cl(1)–C(18)	3.619	$^1/_2 + x, ^1/_2 - y, 1 - z$
Cl(3)–C(3)	3.649	$x, y, 1 + z$
Cl(3)–C(8)	3.643	$x - ^1/_2, 1 - y, ^1/_2 + z$
Cl(3)–C(9)	3.394	$x - ^1/_2, 1 - y, ^1/_2 + z$
Cl(3)–C(13)	3.690	$x - ^1/_2, y, ^1/_2 + z$
Cl(4)–C(2)	3.687	$x, y, 1 + z$
Cl(5)–C(4)	3.622	$^1/_2 + x, ^1/_2 - y, 1 - z$
C(2)–C(12)	3.617	$x, ^1/_2 + y, ^1/_2 - z$
C(3)–C(12)	3.607	$x, ^1/_2 + y, ^1/_2 - z$
C(8)–C(17)	3.584	$x - ^1/_2, ^1/_2 - y, 1 - z$
C(8)–C(18)	3.630	$x - ^1/_2, ^1/_2 - y, 1 - z$
C(9)–C(16)	3.627	$x - ^1/_2, ^1/_2 - y, 1 - z$
C(9)–C(17)	3.635	$x - ^1/_2, ^1/_2 - y, 1 - z$

[a] Cl–Cl ≤ 4.25 Å; Cl–C and C–C ≤ 3.70 Å.

Results and Discussion

Crystal Structure of $[Fe(bpy)_2Cl_2][FeCl_4]$. The crystal structure consists of the packing of discrete $[Fe(bpy)_2Cl_2]^+$ cations and $[FeCl_4]^-$ anions, both of which occupy general positions in space group $P2_12_12_1$. The packing is illustrated as a stereopair in Figure 1. The shortest interionic contact [Cl(3)–C(9)] is 3.394 Å; there are no other intermolecular contacts less than the sum of the appropriate van der Waals radii. However, the results of the magnetic and Mössbauer studies appear to indicate that a number of slightly longer range contacts are important. An examination of the intermolecular contacts provided in Table III reveals a three-dimensional network of anion–anion, anion–cation, and cation–cation contacts at distances somewhat greater than the sum of the van der Waals radii. These contacts serve to interleave the ions throughout the crystal. The $[FeCl_4]^-$ anions are all interconnected via two types of Cl–Cl interaction; Cl(3)–Cl(4) (3.864 Å) interactions relate pairs of $[FeCl_4]^-$ units primarily in the *ac* plane while Cl(5)–Cl(6) (3.735 Å) contacts relate all anions primarily in the *bc* plane. The $[Fe(bpy)_2Cl_2]^+$ units are included in the framework by a series of cation–anion interactions represented by Cl–Cl contacts [Cl(1)–Cl(4) (3.880 Å), Cl(2)–Cl(5) (4.044 Å), and Cl(2)–Cl(6) (4.248 Å)] and by several Cl(anion) to C(cation) contacts of which Cl(3)–C(9) (3.394 Å) is the shortest. Finally, the $[Fe(bpy)_2Cl_2]^+$ cations are interconnected via several C–C and C–Cl contacts, the shortest being 3.584 Å (C(8)–C(17)) and 3.619 Å (Cl(1)–C(18)), respectively. Hence the crystal packing can be viewed as a mixture of two loosely packed $[FeCl_4]^-$ and $[Fe(bpy)_2Cl_2]^+$ systems, which, in turn, are interrelated by C–C, Cl–C and Cl–Cl contacts.

The crystal and molecular structure of a second polymorph of $[Fe(bpy)_2Cl_2][FeCl_4]$, which crystallizes in space group *Pccn*, has been reported.[10] The structures of the molecular anions and

(8) Reiff, W. M.; Cheng, C. *Inorg. Chem.* **1977**, *16*, 2097.
(9) (a) Foxman, B. M. *Inorg. Chem.* **1978**, *17*, 1932–1938. (b) Foxman, B. M.; Mazurek, H. *Inorg. Chem.* **1979**, *18*, 113–116. (c) Scattering factors and corrections for anomalous scattering (Fe, Cl) were taken from: "International Tables for X-ray Crystallography"; Kynoch Press: Birmingham, England, 1974, Vol. IV, pp 99–101 and 148–150.
(10) Figgis, B. N.; Patrick, J. M.; Reynolds, P. A.; Skelton, B. W.; White, A. H.; Healy, P. C. *Aust. J. Chem.* **1983**, *36*, 2043–2055. Figgis, B. N.; Reynolds, P. A.; Lehner, N. *Acta Crystallogr. Sect. B: Struct. Sci.* **1983**, *39*, 711–717.

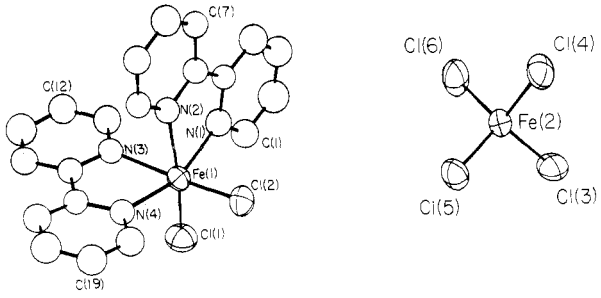

Figure 2. Molecular structure of the $[Fe(bpy)_2Cl_2]^+$ and $[FeCl_4]^-$ ions showing anisotropic temperature factors for iron and chlorine atoms (50% probability ellipsoids).

Table IV. Selected Bond Lengths (Å) and Angles (deg) in $[Fe(bpy)_2Cl_2]^+[FeCl_4]^-$

Fe(1)–Cl(1)	2.252 (4)	Fe(1)–N(4)	2.122 (9)
Fe(1)–Cl(2)	2.258 (4)	Fe(2)–Cl(3)	2.183 (5)
Fe(1)–N(1)	2.120 (10)	Fe(2)–Cl(4)	2.183 (4)
Fe(1)–N(2)	2.198 (10)	Fe(2)–Cl(5)	2.187 (4)
Fe(1)–N(3)	2.188 (10)	Fe(2)–Cl(6)	2.183 (4)
Cl(1)–Fe(1)–Cl(2)	101.6 (2)	N(1)–Fe(1)–N(4)	160.4 (4)
Cl(1)–Fe(1)–N(1)	98.4 (3)	N(2)–Fe(1)–N(3)	81.3 (4)
Cl(1)–Fe(1)–N(2)	167.2 (3)	N(2)–Fe(1)–N(4)	89.0 (4)
Cl(1)–Fe(1)–N(3)	87.9 (3)	N(3)–Fe(1)–N(4)	75.6 (4)
Cl(1)–Fe(1)–N(4)	95.1 (3)	Cl(3)–Fe(2)–Cl(4)	110.1 (2)
Cl(2)–Fe(1)–N(1)	93.4 (3)	Cl(3)–Fe(2)–Cl(5)	109.0 (2)
Cl(2)–Fe(1)–N(2)	89.8 (3)	Cl(3)–Fe(2)–Cl(6)	109.0 (2)
Cl(2)–Fe(1)–N(3)	169.0 (3)	Cl(4)–Fe(2)–Cl(5)	110.2 (2)
Cl(2)–Fe(1)–N(4)	97.8 (3)	Cl(4)–Fe(2)–Cl(6)	108.6 (2)
N(1)–Fe(1)–N(2)	74.9 (4)	Cl(5)–Fe(2)–Cl(6)	110.0 (2)
N(1)–Fe(1)–N(3)	90.7 (4)		

cations do not differ significantly in the two polymorphs; however, the crystal packing is quite different. This latter feature would appear to have a bearing on the different magnetic phenomena observed for the two phases. The unit cell in the present work is 2% larger than that of the *Pccn* polymorph. Both structures contain nearly linear chains of cation···anion···cation. The $P2_12_12_1$ polymorph has an approximately linear cation/anion/cation separation of $\sim c/2$ (see Table II and Figure 1); the angle subtended at Fe is 172.8°. The *Pccn* polymorph has an Fe–Fe–Fe angle of ~161°, with unequal Fe–Fe distances along the chain.

The $[FeCl_4]^-$ ion (Figure 2) displays the expected tetrahedral geometry with an average Fe–Cl bond length of 2.184 (2) Å. The molecular structure of the $[Fe(bpy)_2Cl_2]^+$ ion is also shown in Figure 2, and bond distances and angles are given in Table IV. The coordination of four nitrogen atoms and two chloride ions to the central iron atom produces a distorted octahedron as expected from the geometric requirements of the bipyridyl ligands.

The $[Fe(bpy)_2Cl_2]^+$ cation assumes the cis configuration; a trans configuration without pronounced ligand and/or polyhedron distortions would produce a very unfavorable approach of the two α-hydrogen atoms of opposing bipyridyl ligands.[11] In addition, given the "normalized bite" of the bidentate, which is defined as the distance between the two donor atoms divided by the metal–donor atom bond length, the cis configuration of $[Fe(bpy)_2Cl_2]^+$ is calculated to be stabilized with respect to the trans geometry on the basis of the ligand–ligand repulsion energy.[12]

The average Fe–Cl distance is 2.255 (4) Å, which agrees well with that reported[13] for the similar dichlorobis(1,10-phenanthroline)iron(III) cation (2.258 Å) as well as polymorph 2 of the bpy complex (2.263 Å).[10,13] The Fe–N distance trans to Cl (average 2.193 (7) Å) is significantly lengthened over the Fe–N distance cis to Cl (average 2.121 (9) Å). Again, this result is consistent with the Fe–N bond distances found in the analogous

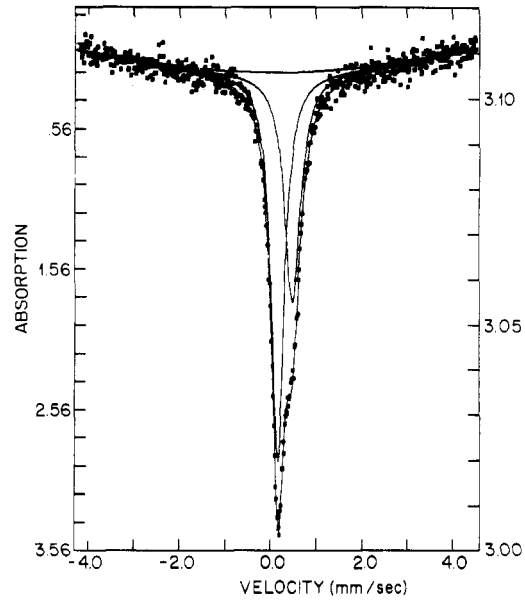

Figure 3. Ambient-temperature Mössbauer spectrum of $[Fe(bpy)_2Cl_2][FeCl_4]$.

phen complex (2.206, 2.136 Å) and the other bpy polymorph (2.176, 2.136 Å).[10,13] Such distortions in Cu(II) complexes have been attributed to Jahn–Teller effects.[14] However, this effect is also present in octahedral d^0 and d^3 complexes as well as in the present high-spin d^5 complex.[15] The distortion may originate from an equalization of nonbonded contacts.[12] We note that the Cl···N contacts are shorter for N(2) and N(3) even though the observed Fe–N lengthening serves to partially alleviate their severity. The bond lengths and bond angles of the bipyridyl ligands are normal.[16]

While the individual pyridyl groups approximate planarity, the bipyridyl systems are distorted from the planarity found in uncoordinated 2,2′-bipyridine. Instead, there is a rotation about the bridging C–C bond of the pyridyl rings with respect to one another. This twist produces dihedral angles between the pyridine moieties equal to 3.18 and 9.15° for the N(1), N(2) and N(3), N(4) ligands, respectively. The magnitudes of these dihedral angles are not unusual for complexed 2,2′-bipyridine; values ranging from 0 to 31° have been observed previously.[17]

Mössbauer Spectra, ESR, and Magnetic Susceptibility Measurements. The Mössbauer spectrum at ambient temperature for a velocity sweep of ±4.5 mm/s is an asymmetric pattern that can be fit to a small quadrupole doublet (δ = 0.418 mm/s, Fe ≡ 0) (ΔE = 0.245 mm/s) corresponding to the distorted cation and a singlet (δ = 0.244 mm/s, Fe ≡ 0) for the nearly T_d anion. An alternative fit for two slightly broadened Lorentzians gives essentially the same isomer shifts and goodness of fit parameter and is shown in Figure 3. In any event the foregoing isomer shift values are clearly characteristic of six- and four-coordinate high-spin iron(III), respectively.[18]

The Mössbauer spectra between 8 and 3 K exhibit the *gradual hyperfine splitting* of one of the ferric species ($H_{internal}$(4.2 K) = 428 kG) for which the absolute value of $H_{internal}$ is *relatively temperature-independent* (see Figures 4 and 5). The observations are clearly consistent with slow paramagnetic relaxation broadening at this site. The strong, unbroadened singlet remaining at 4.2 K has an isomer shift of 0.34 mm/s with respect to natural iron. This value of δ corresponds to tetrahedral Fe(III) after

(11) McKenzie, E. D. *Coord. Chem. Rev.* **1971**, *6*, 187–216.
(12) Kepert, D. L. *Inorg. Chem.* **1973**, *12*, 1944–1949; *Prog. Inorg. Chem.* **1977**, *23*, 1.
(13) Goodwin, H. J.; McPartlin, M.; Goodwin, H. A. *Inorg. Chim. Acta* **1977**, *25*, L74.
(14) Clifford, F.; Counihan, E.; Fitzgerald, W.; Seff, K.; Simmons, C.; Tyagi, S.; Hathaway, B. *J. Chem. Soc., Chem. Commun.* **1982**, 196–198.
(15) (a) Restivo, R.; Palenik, G. J. *J. Chem. Soc., Dalton Trans.* **1972**, 341–344. (b) Daly, J. J.; Sanz, F.; Sneden, R. P. A.; Zeiss, H. H. *J. Chem. Soc. Dalton Trans.* **1973**, 73–76.
(16) Merritt, L. L.; Schroeder, E. D. *Acta Crystallogr.* **1956**, *9*, 801–804.
(17) Durham, B.; Wilson, S. R.; Hodgson, D. J.; Meyer, T. J. *J. Am. Chem. Soc.* **1980**, *102*, 600–607.
(18) Greenwood, N. N.; Gibb, T. C. "Mössbauer Spectroscopy"; Chapman and Hall: London, 1972.

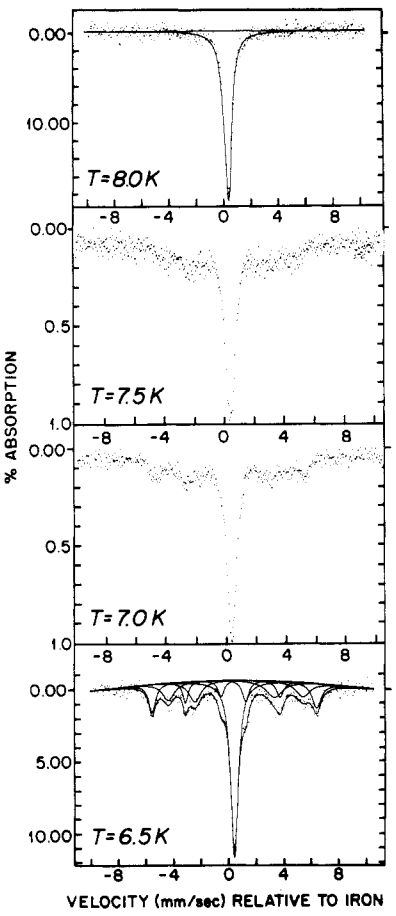

Figure 4. Mössbauer spectra of $[Fe(bpy)_2Cl_2][FeCl_4]$ between 8.0 (top) and 6.0 K (bottom).

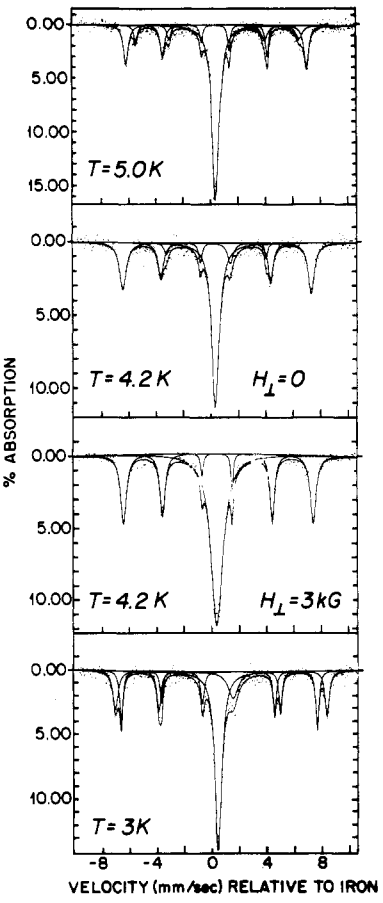

Figure 5. Mössbauer spectra of $[Fe(bpy)_2Cl_2][FeCl_4]$ between 5.0 (top) and 3.0 K (bottom).

extrapolation to room temperature and correction for a second-order Doppler shift of typically ~0.1 mm/s. That is, the *anion* remains as a rapidly relaxing paramagnet at 4.2 K (Figure 5). The cation has lower electronic symmetry than the anion. This apparently leads to zero-field splitting of its sextet and a slowly relaxing ground Kramers doublet. The other requirement for slow paramagnetic relaxation of undiluted high-spin iron(III) compounds is large (≳7 Å) Fe^{3+}---Fe^{3+} separations leading to long spin–spin relaxation times.[19] The shortest separation between cationic centers is 7.519 Å, while individual cation–anion centers are 6.930 Å from one another. The other important "smallest" metal–metal distance is the interanion separation of 7.457 Å. This can also lead to slow paramagnetic relaxation–spectral broadening at the $[FeCl_4]^-$ sites. However, in the absence of distortion and zero-field splitting of their ground spin sextet, such broadening is not expected and indeed is seldom observed at T_D ferric ion sites. In addition to the X-ray data, the essential cubic symmetry of the T_D sites is also indicated by ambient-temperature and 78 K ESR spectra. They show an intense resonance centered at g = 2, typical of $[FeCl_4]^-$. Transitions for the cation were not resolved.

The slow paramagnetic relaxation for the cation is complex to say the least, and quantitative modeling of it is clearly beyond the scope of the present work. In addition, the central transitions of the cation are partially obscured by the anion intensity, precluding detailed modeling. However, the following comments are pertinent. Wickman has considered the complexities of slow paramagnetic relaxation for high-spin iron(III) compounds from experimental and theoretical points of view and for singly[19] and multiply occupied Kramers doublets ($m_s = \pm^1/_2, \pm^3/_2, \pm^5/_2$) of the ground sextet manifold. In summary, for a *singly occupied Kramers doublet* four distinct cases arise:

Case I is uniaxial hyperfine interaction such that $A_z >> A_x = A_y \approx 0$. For a *singly occupied doublet* this leads to a six-line hyperfine pattern having the standard (symmetric) 3:2:1:1:2:3 intensity pattern but for which the γ-ray transitions are not circularly polarized.

Case II is an isotropic hyperfine interaction such that $A_x = A_y = A_z$. This leads to an asymmetric three-transition spectrum for real or pseudo-spin $S = {}^1/_2$ with the asymmetric intensity pattern of 5:1:2.

Case III is an axial symmetry such that $A_z >> A_x = A_y \neq 0$. Case I is a special case of this. For a single Kramers doublet, this leads to a 10-transition spectrum, again with an asymmetric intensity pattern of 6:4:1:1:1:1:2:2:3:3.

Finally there is case IV, anisotropic hyperfine interaction such that $A_z >> A_x > A_y$. Again for a *single Kramers doublet* this leads to a *16*-transition pattern with a *symmetric* intensity pattern of 6:6:4:4:1:1:1:1:1:1:1:1:4:4:6:6.

Save for the velocity region between roughly ~−2.5 and ~+2.5 mm/s (where the anion obscures matters) our limiting spectra (e.g. at 3.0 K) are similar to that predicted by Wickman (case IV), suggesting a highly anisotropic hyperfine interaction.

For the present system, the application of a small *transverse* field induces broadening of the anion singlet and causes shifts of some of the components of the hyperfine pattern. Compare the Mössbauer spectrum taken at H_0 = 0 kG, 4.2 K to that at H_0 = 3 kG, 4.2 K; both are shown in Figure 5. A small external field is expected to increase the paramagnetic relaxation time for the rapidly relaxing anion or alternatively decrease its relaxation rate and initiate broadening. The details of the field dependence for the energy of the components for hyperfine spectra such as considered here have also been discussed by Wickman.[19]

As the compound is cooled below 4.2 K, a second and now very *sharp magnetic hyperfine splitting* process is observed for the strong anion singlet near zero velocity. This occurs between 2.75 and 1.66 K for both the solution recrystallization and thermolytic preparations and leads to the observation of a total of 16 transitions

(19) (a) Wignall, J. W. G. *J. Chem. Phys.* **1968**, *44*, 2462. (b) Wickman, H. H.; Klein, M. P.; Shirley, D. A. *Phys. Rev.* **1966**, *152*, 345–357. (c) Wickman, H. H.; Wertheim, G. K. *Phys. Rev.* **1966**, *148*, 211–217.

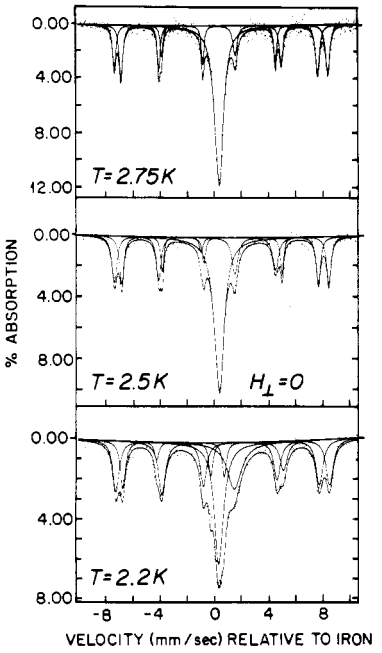

Figure 6. Mössbauer spectra of [Fe(bpy)$_2$Cl$_2$][FeCl$_4$] between 2.75 (top) and 2.2 K (bottom).

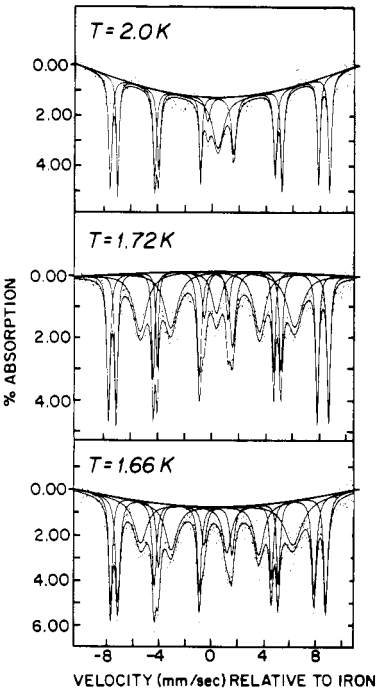

Figure 7. Mössbauer spectra of [Fe(bpy)$_2$Cl$_2$][FeCl$_4$] between 2.0 and 1.66 K.

in the limiting low-temperature Mössbauer spectra, i.e. 12 relatively sharp transitions from the cation on a background of 4 considerably broader transitions from the anion, the paramagnetic singlet phase of the anion having nearly zero intensity at 1.66 K (see Figures 6 and 7). For the present system, the application of a small *transverse* magnetic field (compare the spectrum for H_0 = 0 kG, T = 2.5 K (Figure 6) to that for H_0 = 3.0 kG, T = 2.5 K (Figure 8)) now leads to a significant decrease in the intensity of the central (anion) singlet and additional hyperfine splitting corresponding to ready magnetization of the system and a ferri- or weakly ferromagnetically ordered state. It is expected that, with further decreasing temperature below ~1.6 K, all of the nuclear Zeeman transitions for the ordered anion will resolve and sharpen as magnetic saturation is achieved. Essentially, *coincident* with this nuclear Zeeman splitting is a rapid rise in the magnetic moment μ (Figure 9). These observations taken

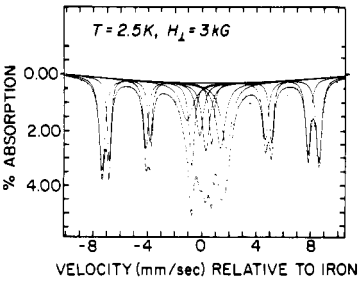

Figure 8. Mössbauer spectra of [Fe(bpy)$_2$Cl$_2$][FeCl$_4$] at 2.5 K. $H_\perp$ = 3 kG.

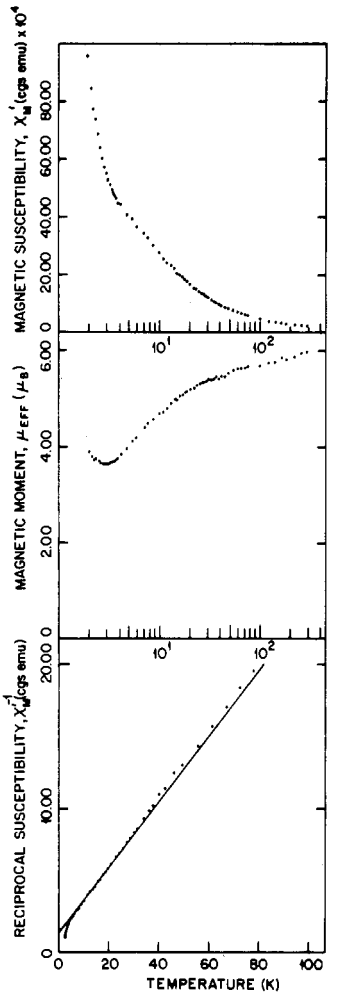

Figure 9. Temperature variation of χ'_M (top), μ (middle) and χ_M^{-1} (bottom) for [Fe(bpy)$_2$Cl$_2$][FeCl$_4$].

together strongly indicate cooperative three-dimensional magnetic ordering. The value of μ (powder sample) has *decreased* from ~5.85 μ_B (i.e., near the spin-only/metal atom value) at 302 K to a minimum of ~3.6 μ_B at 3 K. The Curie–Weiss law parameters resulting from least squares computer fits of $\chi'_M{}^{-1}$ vs. $(T-\Theta)/C$ over the range 40–300 K are μ_{eff} = 5.91 μ_B, Θ = −8.60 K, and C = 4.36 emu/mol. It is clear from Figure 9 (bottom) that a single Curie–Weiss law is not adequate at even lower temperatures. One has a general picture of complex relaxation, weak antiferromagnetic exchange, and moment-decrease behavior whose magnitude cannot be accommodated for by typical single-ion zero-field splitting effects alone.

Discussion

In view of the highly interleaved close contact network nature of the material, one might expect onset of ordering to lead to a molecular field at both the slowly relaxing cation lattice and the anion lattice. The low-temperature magnetic behavior, in particular the unusual and abrupt downward turn of $\chi'_M{}^{-1}$ vs. T, is

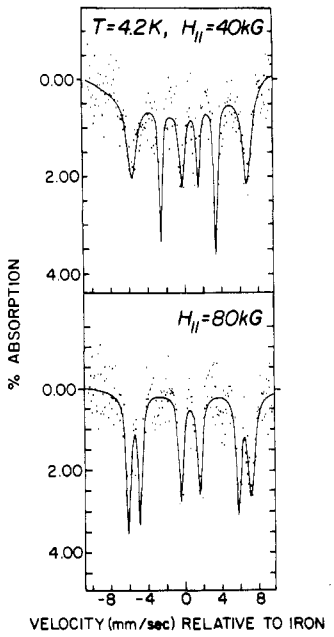

Figure 10. Mössbauer spectra of $[Fe(bpy)_2Cl_2][FeCl_4]$: (top) T = 4.2 K, $H_\parallel$ = 40 kG; (bottom) T = 4.2 K, $H_\parallel$ = 80 kG.

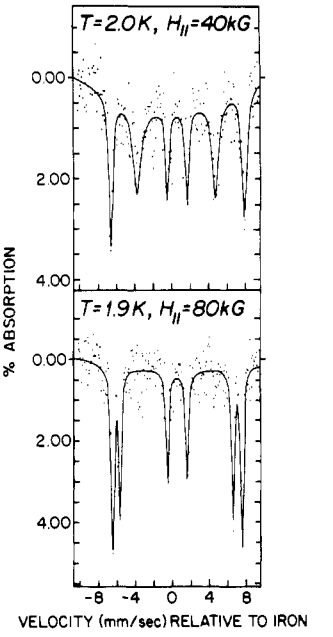

Figure 11. Mössbauer spectra of $[Fe(bpy)_2Cl_2][FeCl_4]$: (top) T = 2.0 K, $H_\parallel$ = 40 kG, (bottom), T = 1.9 K, $H_\parallel$ = 80 kG.

characteristic[20] of overall ferrimagnetic ordering where $T_{critical} \approx$ 2.25 K from the Mössbauer spectra for the material. The metal ion site inequivalence leading to different moments necessary for the latter type of cooperative ordering is obvious. One basically has structurally inequivalent and interpenetrating cation and anion lattices that are highly connected via short nonbonded Cl–Cl contacts.

On the other hand, the zero-field Mössbauer spectra for $T <$ 3 K would seem to suggest that the cation is not involved in the ordering process and is essentially magnetically independent of the anion sublattice. This comment is stimulated by the observation that for the spectra we have determined in this region with the hyperfine splitting of the anion lattice the spectrum of the cation appears little affected. One might have expected some change in this hyperfine spectrum with the spontaneous growth of a molecular field for $T < \sim 2.5$ K. More spectra and significantly lower temperatures need to be determined to clarify this point.

$[Fe(bpy)_2Cl_2][FeCl_4]$ may be similar to $[bpyH][FeCl_4]$ and $[phenH][FeCl_4]\cdot HCl$ save for a considerably lower ordering temperature. We[20] find that the latter bipyridinium and phenanthrolinium systems order *antiferromagnetically* at 4.5 and 3.9 K, respectively, and clearly for these cases all "magnetism" resides in the tetrahedral anion sublattices. Thus for the present system, the paramagnetic $[Fe(bpy)_2Cl_2]^+$ cation may be simply acting as an independent diluent that happens to exhibit very complex slow paramagnetic relaxation for which the hyperfine interaction, A, is highly anisotropic.

In passing we note that there is precedence for complex bimetallic salts in which only one sublattice is apparently ordered. Lambrecht[20] et al. have recently described the low-temperature magnetic properties of $[Co(C_5H_5NO)_6][CoCl_4]$ and find that the hexakis(pyridine *N*-oxide)cobaltous cation exhibits antiferromagnetic ordering at 0.95 K while the tetrachlorocobaltate(II) anion remains a paramagnet to at least 0.04 K. There is however, evidence in the heat capacity data that the tetrahedral anions experience a molecular field from the ordered cation lattice. Figures 10 and 11 are an attempt to further clarify this aspect of the magnetism of $[Fe(bpy)_2Cl_2][FeCl_4]$ via high-field Mössbauer spectroscopy. Now the applied fields are *longitudinal* ($H_0 \| E_\gamma$). In Figure 10, it is seen that for H_0 = 40 kG at 4.2 K slow relaxation has been induced in the anion sublattice while the spectrum of the cation is also clearly simplifying and following the applied field. When H_0 has reached 80 kG, there is significant polarization (alignment parallel to H_0) of the moments of both sublattices as evidenced by the approach of the intensity of the $\Delta m_I = 0$ transitions to zero. (Close examination of the spectrum shows that there is still some residual $\Delta m_I = 0$ transition intensity.) This is exactly the expected limiting behavior for slowly relaxing paramagnetic sublattices in longitudinal fields, since the intensity of the $\Delta m_I = 0$ transitions is proportional to $\sin^2\theta$, where θ is the angle between $H_{internal}$ and $\vec{E}_\gamma$. That is, the progressive application of a field forces $\theta \rightarrow 0$ for various polycrystals. The two sublattices are resolved with the appearance of doublets at the velocity extremes of the H_0 = 80 kG spectrum. A similar set of high-field spectra in the vicinity of ~2 K (Figure 11) and near the presumed ordering temperature shows even further polarization of the sublattice moments and better sublattice resolution at high and low velocities. Note that high-field Mössbauer spectra are not expected to resolve different sublattice components for the $\Delta m_I = -1$ and $\Delta m_I = +1$ transitions just above and just below zero velocity, respectively, especially for a polycrystalline absorber. Applied field spectra between 0 and 40 kG at ~2 K show *no evidence* of a spin–flop transition expected for a simple *antiferromagnet*. Hence the overall high-field behavior near 2 K is consistent with either ferrimagnetism or weak ferromagnetism. The former can arise if, as discussed previously, the cation is involved and one has, for instance, a classical two-sublattice collinear Néel ferrimagnetic. If the cation is indeed *not involved*, one can still have similar overall susceptibility and Mössbauer spectroscopy behavior for noncollinear antiferromagnetic coupling within the anion lattice leading to a net moment and a so-called "weakly ferromagnet state". The presently available susceptibility and Mössbauer data for *polycrystalline* samples do not readily distinguish the preceding possibilities.

In the absence of single-crystal susceptibility and neutron diffraction data all we can say for now about the magnetic structure is that the mechanism of the long-range ordering probably involves the delocalization of metal electron spin density to chloride anion ligands and magnetic exchange via the extensive network of short nonbonded interanion, intercation and anion–cation contacts discussed previously in the X-ray results. Finally, although one view of the structure is that it is chainlike (chains of alternating cations and anions), low dimensionality (1D) effects are not obvious in the present powder susceptibility data or for that matter the Mössbauer results, i.e. reduced hyperfine fields

(20) (a) Cullity, B. D. "Introduction to Magnetic Materials"; Addison-Wesley: Reading, MA, 1972. (b) Reiff, W. M.; Witten, E., unpublished results for $[bpyH][FeCl_4]$ and $[phenH][FeCl_4]\cdot HCl$. (c) Lambrecht, A.; Burriel, R.; Carlin, R. L.; Mennenga, G.; Bartolome, J.; DeJongh, L. J. *J. Appl. Phys.* **1982**, *53*, 1891–1892.

accompanying the reduced spin[21] of a 1D or 2D antiferromagnet. The average value of H_{int} at 1.6 K is ~500 kG. This is a reasonable value for the usual single ion covalency reduction effects, assuming a Fermi contact contribution of 11 T/unpaired electron and negligible dipolar and orbital contributions to H_{int}.

In the present context, it is useful for us to summarize the major conclusions of Figgis et al.'s refinement of polarized neutron diffraction data[22] for the *Pccn* polymorph of $[Fe(bpy)_2Cl_2][FeCl_4]$:

(1) There is ~15% spin delocalization from the iron(III) of the cation, and most of it is to the chlorine ligands.

(2) For the anion the spin delocalization is slightly[24] larger (~17%) and nonspheric.

(3) The site magnetizations for the cation and anion are not equal and have different temperature dependencies.

(4) There is no evidence of extended cooperative magnetic order from the neutron study to 4.2 K.

We believe that metal ion to chlorine ligand spin-delocalization patterns very similar to that in points 1 and 2 and the magnetization behavior (point 3) are undoubtedly operative for the present $P2_12_12_1$ polymorph and are integral to its exchange and ultimate ordering. The nonobservation of clear-cut magnetic ordering in the polarized neutron study[22] of the *Pccn* polymorph is likely related to the fact that only four reflections were studied in detail at the presumed lowest temperature (2.07 K) of the neutron investigation. On the other hand, differences in packing between the two polymorphs might somehow contribute to a somewhat lower critical temperature for the *Pccn* analogue. The susceptibility study[23] of the *Pccn* polymorph leads us to favor the former explanation. Specifically, there is a sharp downward bend of the reciprocal susceptibility (χ_M^{-1}) at ~2.9 K, paralleling that observed by us at ~3.0 K and suggesting the onset of some type of complex magnetic ordering behavior for both polymorphs.

In passing, we also mention that we have performed Mössbauer spectroscopy and susceptibility studies of the phenanthroline analogue, $[Fe(phen)_2Cl_2][FeCl_4]$, which crystallizes in space group $P\bar{1}$ and whose structure has recently been determined[13] and a sample furnished to us. Our helium-4 experiments show that this material exhibits incipient magnetic hyperfine splitting–relaxation broadening effects in its zero-field Mössbauer spectrum at 1.5 K. Preliminary helium-3 studies show that the material is fully hyperfine split at 0.35 K. Complete details for this system will be published subsequently.

Acknowledgment. This work was supported by the NSF DMR Solid State Chemistry Program, Grant Nos. DMR 8016441 and 8313710 (Northeastern University), and by the Office of Naval Research (Brandeis University). W.M.R. thanks Professor H. J. Goodwin of the University of New South Wales for his donation of a sample of the $P\bar{1}$ polymorph of $[Fe(phen)_2Cl_2][FeCl_4]$.

Supplementary Material Available: Tables of least-squares planes, nonessential bond lengths and angles, anisotropic temperature factors, H-atom coordinates, intramolecular nonbonded contacts, and observed and calculated structure amplitudes (12 pages). Ordering information is given on any current masthead page.

(21) Johnson, C. E. "Proceedings of the International Conference on the Applications of the Mössbauer Effect, Jaipur, India"; Indian National Science Academy: New Delhi, 1981; p 72.
(22) Figgis, B. N.; Reynolds, P. A.; Mason, R. *Inorg. Chem.* **1984**, *23*, 1149–1153.
(23) Figgis, B. N.; Kucharski, E. S.; Reynolds, P. A. *Aust. J. Chem.* **1983**, *36*, 2369–2375.
(24) A more recent detailed X-ray study (120 K) (Figgis, B. N.; Reynolds, P. A.; White, A. H. *Inorg. Chem.* **1985**, *24*, 3762) of the *Pccn* polymorph has appeared since the acceptance of the present work. This work suggests *somewhat* larger total spin delocalization to the anion ligands as opposed to the cation ligands. Specifically, there is a total of 0.88 spin delocalized to the anion chlorine atoms vs. 0.60 spin for the cation (0.23 spin/Cl^-), and for the latter, little spin density appears beyond the nitrogen atoms of the bipyridyl ligand rings. These observations are consistent with noninvolvement of the cation in the ordered state, a possibility alluded to earlier in the Discussion.

Contribution from the Department of Chemistry, The Pennsylvania State University, University Park, Pennsylvania 16802

Laser Spectroscopic and X-ray Structural Investigation of Europium(III)–Oxydiacetate Complexes in Solution and in the Solid State

Michael Albin, Robert R. Whittle, and William DeW. Horrocks, Jr.*

Received November 15, 1984

Dye-laser-induced luminescence excitation spectra and excited-state-lifetime measurements on solutions of europium(III) chloride and sodium oxydiacetate (ODA) reveal the presence of three complexes: $Eu(ODA)(H_2O)_7^+$, $Eu(ODA)_2(H_2O)_3^-$, and $Eu(ODA)_3^{3-}$. The X-ray structure of monoclinic $Na_3[Eu(ODA)_3]\cdot 6H_2O$ has been determined (space group *Cc*, a = 17.542 (4) Å, b = 8.474 (2) Å, c = 19.181 (3) Å, β = 111.46 (2)°, Z = 4) and is compared with the known structure for $Na_3[Eu(ODA)_3]\cdot 2NaClO_4\cdot 6H_2O$ (space group *R*32, a = 9.7391 (18) Å, b = 28.2012 (74) Å). The spectroscopic results are consistent with the crystallographic metal ion site symmetries (C_1 and D_3, respectively). The $Eu(ODA)_3^{3-}$ solution species resembles the higher symmetry crystalline form.

Physical techniques applicable to both solid-state and solution phases are important in that they permit a comparison between the structures of molecules in the two states. Such methods allow one to extrapolate to the solution state the structural information obtainable from X-ray crystallography on crystalline materials, provided that the experiment in question is sufficiently sensitive to structural details. Considerable effort has been devoted in this laboratory to the development of laser-excited lanthanide ion luminescence as a probe of structure and dynamics in chemistry and biology.[1,2] In particular we have concentrated on the excitation spectroscopy of the highly luminescent and environmentally sensitive Eu(III) ion.[3] The experiment involves exciting the Eu(III) ion from its nondegenerate $^7F_0$ ground state to one of the excited states of the $4f^6$ electronic configuration, $^5D_0$, $^5D_1$, or $^5D_2$, the first of which is also nondegenerate. This excitation is accomplished by using a tunable pulsed dye laser while the emission corresponding to the $^5D_0 \rightarrow {}^7F_2$ transition is monitored. A variety of types of information are obtainable from these experiments, some of which are indicated in Table I.

(1) Horrocks, W. DeW., Jr.; Sudnick, D. R. *Acc. Chem. Res.* **1981**, *14*, 384–392.
(2) Horrocks, W. DeW., Jr.; Arkle, V. K.; Liotta, F. J.; Sudnick, D. R. *J. Am. Chem. Soc.* **1983**, *105*, 3455–3459.
(3) Horrocks, W. DeW., Jr.; Albin, M. *Prog. Inorg. Chem.* **1984**, *31*, 1–104.
(4) Horrocks, W. DeW., Jr.; Sudnick, D. R. *Science (Washington, D.C.)* **1979**, *206*, 1194–1196.
(5) Albin, M.; Horrocks, W. DeW., Jr. *Inorg. Chem.* **1985**, *24*, 895–900.
(6) Breen, P. J.; Horrocks, W. DeW., Jr. *Inorg. Chem.* **1983**, *22*, 536–540.

0020-1669/85/1324-4591$01.50/0